Journal of Physics: Conference Series **2663** (2023) 012049 doi:10.1088/1742-6596/2663/1/012049

# Alpha clustering in $^{41, 45, 49}Ca^{*}$ nuclei formed in neutron induced reactions

**Manpreet Kaur[1], BirBikram Singh[2], S. K. Patra[3, 4], P. K. Raina[1]**

[1]Indian Institute of Technology Ropar, Rupnagar - 140001, India
[2]Department of Physics, Akal University, Talwandi Sabo - 151302, India
[3]Institute of Physics, Sachivalaya Marg, Bhubaneswar - 751005, India
[4]Homi Bhabha National Institute, Anushakti Nagar, Mumbai - 400085, India

manpreetphys@gmail.com

**Abstract**. The light neutron-rich nuclei play a vital role in nucleosynthesis process and the extent of alpha (α) clustering significantly influence the astrophysical rates. Thus, it is significant to explore the α clustering in these nuclei and in the present work, we have studied the α clustering in $^{41,45,49}Ca^{*}$ nuclei formed in neutron induced reactions within the dynamical cluster decay model (DCM). The results present that with progression towards neutron-rich $^{45}Ca^{*}$ and $^{49}Ca^{*}$ nuclei, there is a significant decrease in the α-cluster preformation factor $P_0$. The inclusion of relativistic mean field theory (RMFT) based microscopic temperature-dependent binding energies (T.B.E.) within DCM, give relatively enhanced α-cluster preformation factor for $^{41,45,49}Ca^{*}$ nuclei compared to the case of macroscopic T.B.E. based upon Davidson mass formula. The cross-section associated with α-cluster emission depicts strong isospin dependence and falls off significantly with increasing neutron number of $Ca^{*}$ nuclei. Further, for the first time, we inculcate the microscopic nuclear potential constructed via folding the standard Fermi form fitted RMFT cluster densities and M3Y nucleon-nucleon interaction within the DCM. The neutron skin thickness of the Ar cluster, complementary to α-cluster, is varied and its effect upon the nuclear interaction potential and α-cluster preformation factor is analysed. The results present that with growing neutron skin of Ar cluster, the α-cluster preformation factor decreases. It explores a strong correlation among the neutron skin thickness and α-cluster preformation factor in light mass $^{41,45,49}Ca^{*}$ nuclear systems.

## 1. Introduction

Clustering is a generic phenomenon, which transcends from the cosmic scale to the sub-nuclear scale. The atomic nucleus exhibits the clustering of nucleons owing to a subtle equilibrium between short range repulsive force, medium range attractive force and long range Coulomb repulsion between protons. Alpha (α) clustering is a distinctive feature of light mass α-conjugate N = Z nuclei, which is palpable from the peaks in the binding energy curve for nuclei having nα type structure [1]. The clustering also manifests in non-alpha conjugate neutron-rich nuclei. The covalent exchange of valence neutrons with α-core, analogous to covalent bonding of electrons in atomic molecules, aids to the stability of neutron-rich nuclei [2].

To study the clustering in nuclei, different nuclear reactions such as quasi-elastic scattering, cluster knockout and cluster transfer etc. act as a potent tool [3]. The recent study of (p, pα) reaction involving α-cluster knockout has been carried out to probe α clustering in the isotopic chain of mid mass Sn nuclei

[4]. The observed gradual decrease in the cross-section with increasing neutron number of Sn nuclei explicates that with evolution of neutron-skin, the α-cluster formation gets supressed in heavy nuclei. Such an interplay between neutron-skin and α-clustering in light nuclei needs to be investigated as these light exotic nuclei exhibit an important role in the nucleosynthesis and the degree of α-clustering can significantly affect the astrophysical reaction rates [5]. Therefore, it is intriguing to examine the isotopic dependence of α-clustering in light nuclei and Ca isotopic chain with magic proton number Z = 20 act as an ideal ground to probe aforementioned interplay. To explore the nuclear clustering several models like generalized two centre cluster model, antisymmetrized molecular dynamics, molecular orbit model, fermionic molecular dynamics, cluster formation model, mean field model etc. have been developed [6, 7]. In the present work, the dynamical cluster decay model (DCM) is used to investigate the clustering aspects in the isotopic chain of Ca nuclei formed in neutron-induced reactions. The clustering features in light mass nuclei had been explored successfully within DCM [8-10].

In the present work, we explore the α-clustering in the decay of $^{41,45,49}Ca^{*}$ nuclear systems formed via neutron-induced reactions at same neutron energy $E_n$ = 14 MeV within DCM. For this, we inculcated the microscopic temperature-dependent binding energies (T.B.E) from relativistic mean field theory (RMFT) replacing the Davidson mass formula based macroscopic T.B.E., as discussed in our previous work [11]. Here, for the first time, we incorporate the microscopic nuclear interaction potential obtained by folding the M3Y nucleon-nucleon interaction with RMFT based cluster densities [12] within the DCM and explore the effect of varying neutron skin thickness of Ar cluster, which is complementary to α-cluster, upon the α-cluster preformation factor. The organization of the paper is as follows. The theoretical framework used is presented briefly in Section 2. The results obtained are discussed in the following section. The summary and conclusion are given the Section 4.

## 2. Methodology

Dynamical cluster decay model (DCM) involves the collective coordinates of mass asymmetry (η) and relative separation (R) between daughter and cluster nuclei [8-10]. The cluster decay or production cross-section in terms of $\ell$-partial waves is:

$$\sigma = \frac{\pi}{k^2}\sum_{l=0}^{l_{max}}(2l+1)P_0P; \qquad k=\sqrt{\frac{2\mu E_{c.m.}}{\hbar^2}} \tag{1}$$

where $P_0$ is the cluster preformation probability and P is penetrability (P) and these denote the η-motion and R-motion, respectively. $\ell_{max}$ is the maximum angular momentum for which the cross-section due to light particles (A ≤ 4) is negligibly small ($\sigma_{LP} \rightarrow 0$). The penetrability P is calculated using WKB approximation and cluster preformation factor $P_0$ is given by:

$$P_0(A_i) = |\psi(\eta(A_i))|^2 \ (2/A)\sqrt{B_{\eta\eta}} \tag{2}$$

obtained via the solution of Schrödinger equation of dynamic flow of mass and charge

$$\left\{-\frac{\hbar^2}{2\sqrt{B_{\eta\eta}}}\frac{\partial}{\partial\eta}\frac{1}{\sqrt{B_{\eta\eta}}}\frac{\partial}{\partial\eta}+V_R(\eta,T)\right\}\Psi_R^{(v)}(\eta) = E_R^{(v)}\Psi_R^{(v)}(\eta) \tag{3}$$

where $B_{\eta\eta}$ is hydrodynamical mass parameter [13] and $V_R(\eta, T)$ is fragmentation potential defined as

$$\begin{aligned} V_R(\eta,T) = &\sum_{i=1}^{2}\left[V_{LDM}(A_i,Z_i,T)\right] + \sum_{i=1}^{2}\left[\delta U_i\right]\exp(-T^2/T_0^2) \\ &+V_c(R,Z_i,\beta_{\lambda i},\theta_i,T)+V_p(R,A_i,\beta_{\lambda i},\theta_i,T)+V_l(R,A_i,\beta_{\lambda i},\theta_i,T) \end{aligned} \tag{4}$$

and $V_c$, $V_\ell$ and $V_P$ denote the Coulomb, centrifugal and nuclear proximity potentials, respectively. $V_{LDM}$ are the temperature-dependent binding energies (T.B.E.) by Davidson mass formula and $\delta U_i$ represent the empirical shell corrections given by Myers- Swiatecki. We have replaced the T.B.E., i.e. first two terms of the Eq. (4), by inclusion of microscopic T.B.E. from RMFT with NL3 parameter set [14,15]. The RMFT Lagrangian is solved using the variational method and employing the mean field approximation to get the equations of motion for the nucleons and Bosons field. The temperature enters the formalism via occupation number $n_i$ given as [15]:

$$n_i = v_i^2 = \frac{1}{2}\left[1 - \frac{\varepsilon_i - \lambda}{\tilde{\varepsilon}_i}[1 - 2f(\tilde{\varepsilon}_i, T)]\right] \quad \ldots.(5)$$

where

$$f(\tilde{\varepsilon}_i, T) = \frac{1}{(1 + \exp[\ \tilde{\varepsilon}_i / T])} \quad \ldots(6)$$

is the Fermi-Dirac distribution for the quasi particle energy. The set of coupled differential Eqs. are solved which provide the temperature-dependent binding energies, radii, densities etc.

The neutron and proton densities of clusters are taken in the standard Fermi forms $\rho_{ip}(r_i) = \rho^0_{ip}/[1 + \exp[(r_i - c_i)/a]$ and $\rho_{in}(r_i) = \rho^0_{in}/[1 + \exp[(r_i - c_i)/a]$. The values of $\rho^0_{ip}$ and $\rho^0_{in}$ are fixed by the integration of density distribution which reproduces the proton and neutron numbers, respectively. The surface thickness a = 0.54 and half-radius $c_i = 1.07A_i^{1/3}$ fm are taken from [16], which gives matter radius of heavy nuclei as $R_{rms} = 1.2\ A_i^{1/3}$ fm. The temperature-dependent cluster densities and M3Y nucleon-nucleon interaction are folded together [17] and incorporated within DCM to calculate the microscopic nuclear potential. The subsequent effect of these inculcations upon the α-cluster preformation probability $P_0$ is investigated.

## 3. Results and discussion

In this section, the clustering aspects in the decay of $^{41,45,49}Ca^*$ formed in the (n, α) reactions with incident neutron energy $E_n$ = 14 MeV are discussed. The fragmentation potential governs the probability of preformation of different clusters since lesser the magnitude of fragmentation potential (see Figure 1(a)) more is the preformation factor of the particular mass cluster. The preformation probability of different light clusters within $^{41,45,49}Ca^*$ nuclei is shown in Figure 1(b). We note that 1n is the most probable for all nuclei under study and $^2$H, $^3$H and $^4$He are other probable clusters for $^{41}Ca^*$. While progressing towards the neutron-rich nuclear systems ($^{45}Ca^*$ and $^{49}Ca^*$), the 2n and 3n become more probable and the preformation probability of α-cluster ($^4$He) decreases significantly from $^{41}Ca^*$ to $^{49}Ca^*$ case.

To further explore the α-clustering, we inculcated the RMFT based microscopic (mic) T.B.E. within DCM, which are more reliable compared to Davidson mass formula based macroscopic (mac) T.B.E. The underlying significance of mic T.B.E. compared to mac T.B.E. is discussed in our previous work [11]. T.B.E. are the essential ingredient of fragmentation potential, which is an important input to Schrödinger equation used to evaluate the preformation probability of various clusters within the composite nuclear system. Consequently, T.B.E. carries its footprints in $P_0$ calculations through fragmentation potential. Figure 2(a) depicts the mass dependence of α-cluster preformation

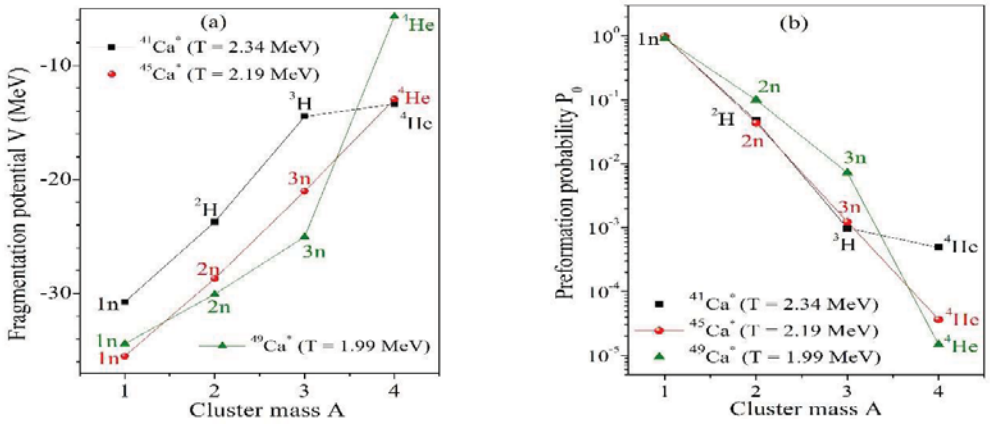


Figure 1: (a) Fragmentation potential (b) preformation probability $P_0$ of different light clusters for $\ell = 0\hbar$ in the $^{41,45,49}Ca^*$ nuclei at temperature corresponding to experimental excitation for $E_n$ = 14 MeV.

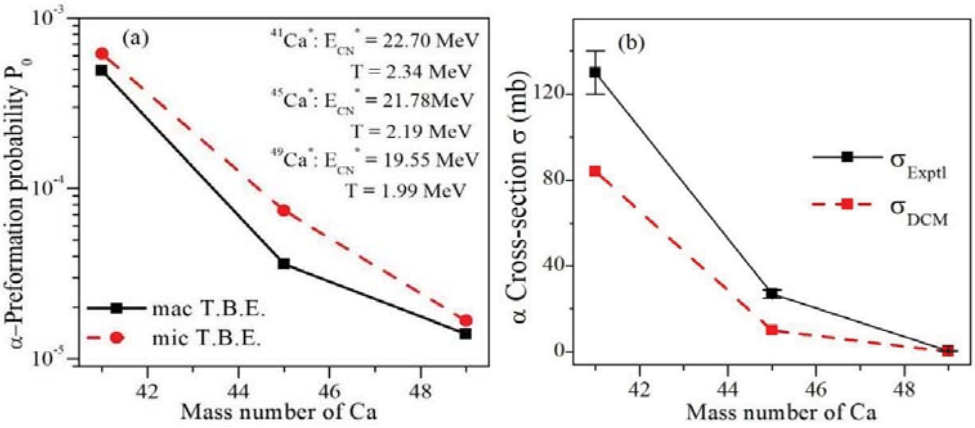


Figure 2: (a) Mass dependence of α-cluster preformation probability $P_0$ for $^{41,45,49}Ca^*$ at $\ell = 0\hbar$ for microscopic T.B.E. and macroscopic T.B.E. cases (b) Mass dependence of α cross-section within DCM using microscopic T.B.E. ($\sigma_{DCM}$) and comparison with experimental data ($\sigma_{Exptl}$).

probability $P_0$ for mac T.B.E. and mic T.B.E. cases, comparatively. It is noted that for the case of mic T.B.E., α-cluster $P_0$ is enhanced comparatively. Depending upon their tunnelling probability across the Coulomb barrier, the α-cluster contribute towards the total cross-section. The cross-section associated with α-cluster emission is calculated for mic T.B.E. case and comparison is made with the available experimental data [18] (see Figure 2(b)). We note that mass dependence of α cross-section follows the same trend as in case of α-cluster $P_0$ advocating that preformation factor encompasses the underlying nuclear structure information.

Further, we probe the dependence of α-cluster preformation probability upon the varying neutron skin thickness of Ar (which is complementary to α-cluster). For this, the neutron and proton densities of clusters are fitted in the standard Fermi forms as discussed in the methodology section. The neutron half-density radius ($c_i$) of $^{37,41,45}Ar$ is changed in steps while the density distribution of proton and other quantities remain unchanged. This gives the varying neutron skin of $^{37,41,45}Ar$. The normalization with respect to neutron number i.e. $\int\rho_n(r)\,dr = 37$, 41 and 45 is also checked for $^{37}Ar$, $^{41}Ar$ and $^{45}Ar$, respectively. The microscopic nuclear interaction potential is calculated for varying

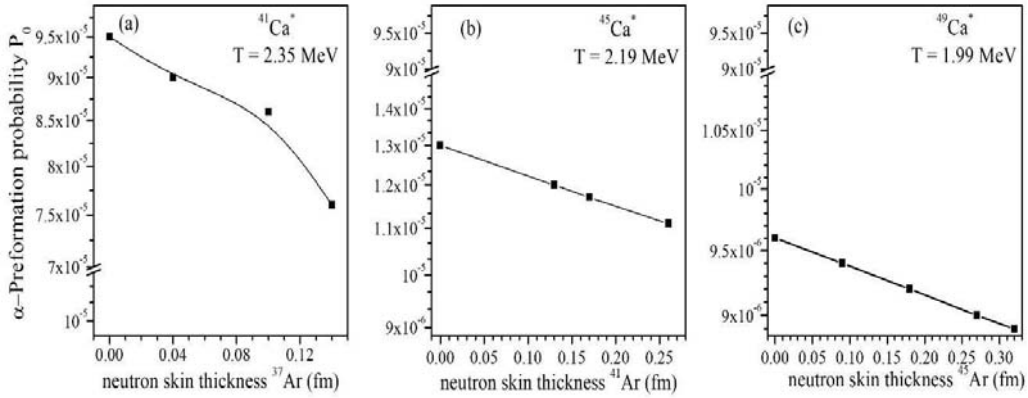


Figure 3: Variation of α-cluster preformation probability $P_0$ with neutron skin thickness of (a) $^{37}Ar$ (b) $^{41}Ar$ and (c) $^{45}Ar$ for the $^{41,45,49}Ca^*$ nuclei at temperature corresponding to experimental energy.

neutron skin of Ar nuclei and it affects the fragmentation potential being an essential ingredient (see Eq. (4)). This fragmentation potential further acts as a key input in the solution of Schrodinger the α-cluster preformation probability. In other words, the effect of varying neutron skin is carried over in preformation probability calculations via fragmentation potential. Figure 3 depicts that with an evolution of neutron skin, there is a reduction in α-cluster preformation probability in $^{41,45,49}Ca^{*}$ nuclei portraying a correlation among them. It apparently happens due to change in the strength of attractive nuclear potential with growing size of neutron-rich nuclei, since the interaction potential is the key factor to calculate the fragmentation potential and hence the cluster preformation probability. Further, the effect of varying neutron skin upon tunnelling across the barrier and α cross-section is under progress.

## 4. Summary

We have investigated the α-clustering in $^{41,45,49}Ca^{*}$ nuclei formed via neutron induced reactions with neutron energy $E_n$ = 14 MeV within the dynamical cluster decay model (DCM). Among the light clusters, 1n is the most probable followed by $^{2}H$, $^{3}H$ and $^{4}He$ for $^{41}Ca^{*}$. For neutron-rich $^{45,49}Ca^{*}$ nuclei, 2n and 3n clusters comes into the picture and here the α-cluster preformation probability $P_0$ drops significantly compared to $^{41}Ca^{*}$. With the inclusion of relativistic mean field theory based microscopic T.B.E. within DCM, the α-cluster preformation probability $P_0$ value increases compared to Davidson mass formula macroscopic T.B.E. The cross-section associated with α-cluster emission also falls off rapidly with increasing neutron number of the $Ca^{*}$ nuclei. This trend is similar to as noted for α-cluster preformation factor $P_0$ which advocates that preformation factor contains the essential nuclear structure information. Further, the variation of the neutron skin thickness of Ar cluster, complementary to α-cluster, has significant influence upon the α-cluster preformation probability $P_0$ and results present a strong correlation between the neutron skin thickness and α-cluster preformation probability for these light mass $^{41,45,49}Ca^{*}$ nuclear systems.

**Acknowledgement**

M. K. acknowledges the support by Science and Engineering Research Board, New Delhi in the form of NPDF vide no. PDF/2021/003191.

## References

[1] Ikeda K, Tagikawa N, Horiuchi H 1968 *Prog. Theor. Phys. Suppl.* ***E*68** 464
[2] Oertzen W V, Freer M, Kanada-En'yo Y 2006 *Phys. Rep.* **432** 43
[3] Hodgson P E, Běták E 2003 *Phys. Rep.* **374** 1
[4] Tanaka J, Yang Z, Typel S, Adachi S *et al.* 2021 *Science* **371** 260
[5] Bardayan DW (2023) *Front. Phys.* **11** 1123868
[6] Liu Y, Ye YL 2018 *Nucl Sci Tech* **29** 184; Ahmed S M S, Yahaya R, Radiman S, Yasir MS *et al.* 2015 *Eur. Phys. J. A* **51** 13
[7] Feldmeier H, Schnack J, 2000 *Rev. Mod. Phys.* **72** 655; Arumugam P *et al*. 2005 *PRC* **71** 064308
[8] Kaur M, Singh B B, Patra S K, Gupta R K 2017 *Phys. Rev. C* **95** 014611
[9] Kaur M, Singh B B, Gupta R K 2019 *Phys. Rev. C* **99** 014614
[10] Kaur M, Singh B B, Patra S K 2021 *AIP Conf. Proc.* **2352** 050022; ibid 2018 *AIP Conf. Proc.* **1953** 140113
[11] Kaur M, Singh B B, Patra S K 2021 *Phys. Rev. C* **103** 054608
[12] Sahoo T, Kaur M, Panda R N, Patra S K 2019 *Int. J. of Mod. Phys. E* ***28*** 1950095
[13] Kröger H, Scheid W 1980 *J. Phys. G* **6** L85
[14] Furnstahl R J, Serot B D, Tang H B 1996 *Nucl. Phys. A* **598** 539
[15] Kaur M, Quddus A, Kumar A, Bhuyan M, Patra S K 2020 *Nucl. Phys. A* **1000** 121871; ibid 2020 *J. Phys.G: Nucl. Part. Phys.* **47** 105102
[16] Walecka J D, 1995 *Theoretical Nucl. Phys. and Subnuclear Phys* Oxford University Press, UK
[17] Kobos A M, Brown B A, Hodgson P E, Satchler G R 1982 *Nucl. Phys. A* **384** 65
[18] Csikai J, Semkova V, Dóczi R *et al.* 1997 *Fusion Engg. and Design* **37** 65